AGU PUBLICATIONS

JGR

Journal of Geophysical Research: Space Physics

RESEARCH ARTICLE
10.1002/2014JA020367

Key Points:
- First systematic investigation of Saturn's high-latitude polar cap boundary
- The PCB is observed poleward of the auroral field-aligned current region
- The southern polar cap boundary is somewhat ordered by the SH PPO phase

Correspondence to:
S. L. Jinks,
sj112@le.ac.uk

Citation:
Jinks, S. L., et al. (2014), Cassini multi-instrument assessment of Saturn's polar cap boundary, *J. Geophys. Res. Space Physics*, *119*, 8161–8177, doi:10.1002/2014JA020367.

Received 8 JUL 2014
Accepted 13 SEP 2014
Accepted article online 18 SEP 2014
Published online 13 OCT 2014

Cassini multi-instrument assessment of Saturn's polar cap boundary

S. L. Jinks[1], E. J. Bunce[1], S. W. H. Cowley[1], G. Provan[1], T. K. Yeoman[1], C. S. Arridge[2,3], M. K. Dougherty[4], D. A. Gurnett[5], N. Krupp[6], W. S. Kurth[5], D. G. Mitchell[7], M. Morooka[8], and J.-E. Wahlund[9]

[1]Department of Physics and Astronomy, University of Leicester, Leicester, UK, [2]Mullard Space Science Laboratory, University College London, Dorking, UK, [3]Centre for Planetary Sciences at UCL/Birkbeck, London, UK, [4]Blackett Laboratory, Imperial College London, London, UK, [5]Department of Physics and Astronomy, University of Iowa, Iowa City, Iowa, USA, [6]Max-Planck-Institut für Sonnensystemforschung, Göttingen, Germany, [7]Applied Physics Laboratory, Johns Hopkins University, Laurel, Maryland, USA, [8]Laboratory for Atmospheric and Space Physics, University of Colorado Boulder, Boulder, Colorado, USA, [9]Swedish Institute of Space Physics, Uppsala, Sweden

Abstract We present the first systematic investigation of the polar cap boundary in Saturn's high-latitude magnetosphere through a multi-instrument assessment of various Cassini in situ data sets gathered between 2006 and 2009. We identify 48 polar cap crossings where the polar cap boundary can be clearly observed in the step in upper cutoff of auroral hiss emissions from the plasma wave data, a sudden increase in electron density, an anisotropy of energetic electrons along the magnetic field, and an increase in incidence of higher-energy electrons from the low-energy electron spectrometer measurements as we move equatorward from the pole. We determine the average level of coincidence of the polar cap boundary identified in the various in situ data sets to be 0.34° ± 0.05° colatitude. The average location of the boundary in the southern (northern) hemisphere is found to be at 15.6° (13.3°) colatitude. In both hemispheres we identify a consistent equatorward offset between the poleward edge of the auroral upward directed field-aligned current region of ~1.5–1.8° colatitude to the corresponding polar cap boundary. We identify atypical observations in the boundary region, including observations of approximately hourly periodicities in the auroral hiss emissions close to the pole. We suggest that the position of the southern polar cap boundary is somewhat ordered by the southern planetary period oscillation phase but that it cannot account for the boundary's full latitudinal variability. We find no clear evidence of any ordering of the northern polar cap boundary location with the northern planetary period magnetic field oscillation phase.

1. Introduction

The question of whether the rapidly rotating gas giant magnetospheres of Jupiter and Saturn are magnetically "open" to the solar wind has been a matter of some debate since the first spacecraft visited them in the 1970s. In rotation-dominated magnetospheres, the Dungey cycle-driven magnetosphere picture which dominates the terrestrial system [*Dungey*, 1961] is assumed to be less important, and an alternative internally driven process (involving no open magnetic field lines) known as the Vasyliunas cycle, originally proposed for Jupiter by *Vasyliunas* [1983], is suggested to be the mechanism which transports the main bulk of internally generated plasma mass out of the system via plasmoid ejection down the magnetotail. To date, there has been no systematic study of the "open-closed field line boundary" at either Jupiter or Saturn, and until the NASA Juno spacecraft arrives at Jupiter in mid-2016, there will be no in situ high-latitude observations available at that planet.

In the Earth's magnetosphere, however, the concept of the open-closed field line boundary or "polar cap boundary" is well understood and has been studied using a variety of instrumental techniques. As the Earth's magnetosphere is strongly driven by the solar wind interaction, determination of the open-closed field line boundary latitudinal motion provides information on the balance of dayside and nightside magnetic reconnection in the system (as described by *Siscoe and Huang* [1985] and *Cowley and Lockwood* [1992, 1996]). A variety of proxies can be used to determine the location of the open-closed field line boundary including the identification of: a cutoff in high-energy (few keV) electron precipitation associated with a trapped population on closed field lines [*Evans and Stone*, 1972]; a nightside ionosphere boundary between diffuse and discrete auroral emission [e.g., *Milan et al.*, 2003]; a boundary in the spectral width echoes from

high-frequency, coherent scatter radars such as Super Dual Auroral Radar Network [e.g., *Chisham et al*., 2004]; elevated electron temperatures within the auroral oval using the European Incoherent Scatter radar facility [e.g., *Hubert et al*., 2010]. *Wild et al*. [2004] caution, however, that care is taken in the use of these approaches as they do not appear to be applicable at all magnetic local times, or across multiple wavelengths (in the case of the auroral imaging). In addition, *Clausen et al*. [2013] have determined that the maximum Region 1 current (i.e., upward directed field-aligned current) as determined by Active Magnetosphere and Planetary Electrodynamics Response Experiment (AMPERE) is colocated to within 1° of the particle precipitation polar cap boundary determined from Defense Meteorological Satellite Program (DMSP) at all magnetic local times. As such the Region 1 current system acts as a reliable proxy for the open-closed field line boundary at Earth.

At Saturn, the NASA/European Space Agency/Agenzia Spaziale Italiana Cassini spacecraft has been gathering data for ~10 years, including significant intervals when the spacecraft trajectory is inclined to the equator, allowing high-latitude magnetosphere observations. The first high-latitude phase was between mid-2006 to mid-2007, the second phase in 2008 and early 2009, and the third phase in early 2013. Key observations have been made of the auroral field-aligned current systems and associated plasma boundaries by various individual or dual in situ data sets [e.g., *Bunce et al*., 2008a; *Talboys et al*., 2009a, 2009b, 2011; *Schippers et al*., 2012]. Additional knowledge of the open-closed field line boundary has been inferred from auroral imaging studies [e.g., *Badman et al*., 2005].

The open-closed field line boundary is a strict and definite division between open and closed field lines. The question is to what extent, or with what certainty, this can be identified in the data. There is a set of signatures indicative of a high-latitude boundary that we will call the polar cap boundary, but we note that some interior flux might be extended closed flux that cannot be distinguished experimentally from open flux (see discussion by *Bunce et al*. [2014]).

Prior to Cassini's arrival at Saturn, *Cowley et al*. [2004] proposed a model to describe the large-scale flows and currents in Saturn's magnetosphere. This model involves a combination of (a) the effects due to plasma mass loading and subcorotation [*Hill*, 1979], (b) mass loss processes associated with plasmoid ejection down tail, as first discussed for Jupiter by *Vasyliunas* [1983], and (c) a modified Dungey cycle process involving reconnection at the magnetopause and in the tail. The *Cowley et al*. [2004] theoretical model suggested a nonmonotonic angular velocity profile (based on V-1 and V-2 data) that with increasing distance first fell from rigid corotation, then rose again in the outer magnetosphere, and then fell again to ~30% precipitately at the open-closed field line boundary, and remained at that in the polar cap. Within the polar cap region, *Cowley et al*. [2004] suggested that the plasma flow consists of a slow ~200 m s^{-1} antisunward motion driven by the solar wind, combined with a strongly subcorotational circulation (at ~30% of rigid corotation) driven by the atmospheric torque, which tends to twist the tail lobe flux tubes [*Isbell et al*., 1984]. *Stallard et al*. [2004] conducted measurements of Saturn's ionospheric flows using ground-based measurements of infrared emissions which broadly agree with a slow rotation of Saturn's polar regions and are thus consistent with the interpretation that the polar cap is open to the solar wind antisunward flow, combined with planetary rotation.

Hence, with a constant conductivity, there are two principle regions of upward field-aligned current, and in the model, the upward directed field-aligned current was stronger/sharper at the open-closed field line boundary. The field-aligned current producing the main oval discussed by *Cowley et al*. [2004, 2008] is associated with a strong lagging azimuthal magnetic field on open polar cap field lines which drops sharply to smaller values on "closed" field lines as the plasma angular velocity rises toward corotation across the boundary. *Cowley et al*. [2004] predicted that an intense layer of upward directed field-aligned current, associated with the change in plasma angular velocity, occurs at the open-closed field line boundary typically located at ~15° colatitude.

Recently, however, G. J. Hunt et al. (Field-aligned currents in Saturn's southern nightside magnetosphere: Auroral region current sheet modulation by planetary period oscillation phase, submitted to *Journal of Geophysical Research*: *Space Physics*, 2014, hereinafter referred to as Hunt et al., submitted manuscript, 2014) have combined the latest information on the angular velocity measurements using Cassini plasma instruments in Saturn's magnetosphere [e.g., *Wilson et al*., 2009; *Müller et al*., 2010; *Carbary and Mitchell*, 2014; *Thomsen et al*., 2014] and have devised a simple empirical model of the angular velocity which reflects the latest observations. Hunt et al. (submitted manuscript, 2014) thus present an overall empirical model of

the plasma angular velocity which consists of a simple monotonic decrease from rigid corotation to 30% of corotation at the open-closed field line boundary. In the absence of further new information about the rotation in the polar cap itself, it is also assumed to subcorotate at ~30% of rigid corotation (as per the *Stallard et al*. [2004] results discussed above). Therefore, assuming a constant conductivity in the ionosphere, this work indicates a single sheet of field-aligned current just equatorward of the open-closed field line boundary (quite similar to that proposed by *Cowley et al*. [2004]). However, it is proposed by Hunt et al. (submitted manuscript, 2014) that the most significant difference in the field-aligned current profile in the ionosphere is associated with changes in the conductivity with latitude.

Notwithstanding the precise details of the angular velocity profile as function of radial distance/ionospheric colatitude, for an equatorial region of plasma subcorotation, leading to a lagging field configuration, where the angular velocity of the neutral upper atmosphere in the Pederson layer, $\Omega^*_S >$ the angular velocity of a particular shell of field lines, ω, the ionospheric electric field in the neutral atmosphere rest frame, and hence, the ionospheric Pedersen current is directed equatorward (taken positive) in both hemispheres. The associated field-aligned currents are then directed upward out of the ionosphere at the inner edge and downward into the ionosphere at the outer edge of the plasma subcorotation regime. The closure currents in the magnetosphere are directed approximately radially outward. The azimuthal magnetic field, B_φ, is given by Ampère's law in the region between the ionosphere and the magnetospheric closure current as

$$B_\varphi = \mp(\mu_o I_P)/\rho, \tag{1}$$

and is positive in the southern hemisphere and negative in the northern hemisphere. In this equation ρ is the perpendicular distance from the axis of symmetry, I_P is the ionospheric Pedersen current per radian of azimuth flowing at the footprint of the magnetic field lines considered, and μ_o is the vacuum permeability. Should some dynamical process cause supercorotation, where $\Omega^*_S < \omega$, the field perturbation would reverse into a leading configuration, with B_φ positive in the northern hemisphere and negative in the south.

The highly inclined orbits of the Cassini mission have provided the first opportunity to study Saturn's high-latitude magnetosphere through in situ measurements of the field-aligned current systems [e.g., *Bunce et al*., 2008a; *Talboys et al*., 2009a, 2009b, 2011]. *Talboys et al*. [2009b] have categorized the direct signatures of auroral field-aligned currents from magnetic field data in Saturn's nightside magnetosphere during 40 orbits in 2008. They identified two types of field-aligned current morphologies associated with a combination of leading and lagging field configurations. "Type 1" azimuthal perturbation field signatures are consistent with that of a lagging field configuration. These were seen in ~65% of the periapsis passes surveyed and were detected by Cassini as a downward-upward directed field-aligned current pair in both the northern and southern hemispheres as the spacecraft moved equatorward from the open polar cap region. "Type 2" were observed ~25% of the time and exhibited signatures consistent with both leading and lagging field configurations. The Type 2 signatures consist of an upward directed field-aligned current region, bordered by two regions of downward current. *Talboys et al*. [2011] presented a statistical study of the characteristics of field-aligned currents in the nightside magnetosphere and also identified the open-closed field line boundary using data from the Cassini Plasma Spectrometer electron spectrometer (CAPS/ELS). They found that the upward directed field-aligned currents associated with the aurora are typically located within the outer magnetosphere on closed field lines rather than at the boundary itself as suggested by the *Cowley et al*. [2004] model. However, *Bunce et al*. [2008a] showed that, in a near-noon example from 2007, the upward directed field-aligned current lies near to the open-closed field line boundary and that this mapped directly to the auroral oval imaged near-simultaneously by the Hubble Space Telescope (HST).

Gurnett et al. [2010] have also identified indications of the open-closed field line boundary in auroral hiss emissions observed in the Cassini Radio and Plasma Wave Science (RPWS) instrument data, and in low-energy electron density data derived from the RPWS Langmuir Probe (LP) observations (the LP proxy method is fully explained in *Morooka et al*. [2009] and further discussed below). They reported the existence of a "plasmapause-like density boundary" at high latitudes in Saturn's magnetosphere. The first indication of this density boundary at Saturn came from observations of auroral hiss, which is a whistler mode emission frequently observed in Earth's polar regions [e.g., *Gurnett*, 1966; *Persoon et al*., 1988; *Kasahara et al*., 1995]. Auroral hiss is also present in Saturn's magnetosphere, usually up to ~100 Hz, generated by upward moving field-aligned electron beams [*Kopf et al*., 2010]. The emission exhibits an upper cutoff frequency at the electron plasma frequency [*Kopf et al*., 2010], and hence, the local electron

density can be measured. Correspondingly, *Gurnett et al*. [2010] showed that an upward step in the cutoff frequency corresponds to an upward step in the electron density in the RPWS/LP data, as Cassini moved equatorward through the density boundary.

To identify the open-closed field line boundary in relation to the plasmapause-like density boundary, *Gurnett et al*. [2010] examined the anisotropy of energetic electrons measured by two telescopes of the Cassini Magnetospheric Imaging Instrument, specifically the Low Energy Magnetospheric Measurement System (MIMI/LEMMS). Due to spacecraft attitude during the interval studied by *Gurnett et al*. [2010], Channels C5 (detecting 175–300 keV electrons) and E0 (detecting 110–365 keV electrons) of the LEMMS telescopes were oriented so that they detected ~200 keV electrons traveling in opposite directions along magnetic field lines. In regions where the electron intensity is approximately the same in both LEMMS channels, the data are interpreted as an indication of closed magnetic field lines, i.e., a magnetically trapped electron population. Conversely, in regions where the intensity of electrons moving upward from the ionosphere, measured by channel C5, is significantly larger than the intensity of electrons moving downward toward the ionosphere, measured by channel E0, i.e., where no electrons are returning from magnetic mirror points in the opposite hemisphere, the data can reasonably be interpreted as an indication of open magnetic field lines.

In the cases of the northern and southern boundary crossings during Cassini's Revolution (Rev) 81 about Saturn, which are shown by *Gurnett et al*. [2010], this open-closed field line boundary is seen to be coincident with the plasma density boundary, which suggests that the LP density boundary and the anisotropy in the LEMMS electron intensity channels can be used as proxies of the boundary location. Both the examples shown by *Gurnett et al*. [2010] identify the open-closed field line boundary at exactly the same location as those inferred by *Talboys et al*. [2011] using the CAPS/ELS electron data. Although identification of the boundary for these two examples seems to be in good agreement, further work is required to determine whether systematic agreement exists across the entire high-latitude data set.

As well as the basic colocation (or otherwise) of the polar cap boundary in the various data sets, we also wish to address the issue of the boundary latitudinal variation with time. This has been previously inferred from ultraviolet (UV) auroral observations of the southern hemisphere, while the Cassini spacecraft was en route and upstream of Saturn in the solar wind [*Badman et al*., 2005]. This study assumed that the poleward edge of the main UV emission was a proxy for the open-closed field line boundary, and investigated the latitude variation of the boundary as a function of the upstream solar wind conditions. It was proposed that the variation in the "reconnection voltage" available to Saturn's magnetosphere from the interplanetary magnetic field played a significant role in the amount of open flux present in Saturn's magnetosphere (indicated by the size of the polar cap), particularly during corotating interaction regions compressions of the magnetosphere. Evidence of solar wind-driven flux transport in Saturn's outer magnetosphere associated with bursty reconnection at the magnetopause [*Badman et al*., 2006, 2013; *Radioti et al*., 2011] also indicates that the location of the polar cap boundary is also likely to exhibit variation due to solar wind coupling effects. Unfortunately, during this interval we have no upstream solar wind monitor and thus cannot consider the solar wind influence on the location of the polar cap boundary.

Instead, here we aim to compare the location of the polar cap boundary with the phase of the "planetary period oscillations" (PPO) which have been found to dominate the dynamics of Saturn's magnetosphere, control the location of the UV and IR auroral oval, and modulate the Saturn Kilometric Radiation (SKR) and auroral hiss emissions [see *Carbary and Mitchell*, 2013, and references therein]. Both the SKR and in situ magnetic field data show evidence that the modulations have a different period in the northern hemisphere, compared to the south [*Gurnett et al*., 2009; *Andrews et al*., 2010; *Lamy*, 2011; *Provan et al*., 2011].

Nichols et al. [2008] showed that the southern auroral oval oscillates with a period close to that of the "planetary period" magnetospheric phenomena via analysis of UV images of Saturn's aurora from the Hubble Space Telescope (HST). They suggested that the aurora-producing upward field-aligned current is modulated by the southern PPO phase, which was later supported by the analysis of *Provan et al*. [2009b] of the relation of the magnetic field oscillation phase to the auroral oval's oscillation. *Gurnett et al*. [2011] showed that the plasmapause-like density boundary at Saturn varies with a phase which matches the motion of the auroral oval, and therefore the PPO phase, of the relevant hemisphere. The morphological difference between the Type 1 and Type 2 field-aligned current systems measured by *Talboys et al*. [2009b] has been suggested to be related to the PPO phases [*Bunce*, 2012].

It is clear then that we need to deduce the relationship between the PPO phases and the associated large-scale current system involving the auroral field-aligned currents [*Bunce et al*., 2008b; *Talboys et al*., 2009a, 2009b, 2011] before we can fully comprehend the complexities and dynamics of Saturn's auroral region. Therefore, consideration is also required of the effect of the PPO on the polar cap boundary location.

Previous work discussed above has shown that one can identify the polar cap boundary from individual Cassini in situ data sets. For the first time here, then, we systematically investigate the location of the polar cap boundary in all of the available in situ data sets, for all of the high-latitude boundary region crossings between 2006 and 2009. For both hemispheres, we determine the level of coincidence between different instrument data sets and hence the average colatitude of the polar cap boundary. We also examine the relative location of the polar cap boundary to the aurora-producing upward field-aligned currents and investigate the relationship between the polar cap boundary location and the northern and southern PPO phases. Since all our observations are nightside and made close to Saturn equinox, we discount local time effects and do not expect any seasonal variation dependence on the polar cap boundary between the northern and southern hemispheres.

2. Multi-instrument Assessment of the Polar Cap Boundary

From Cassini's ~70 high-latitude orbits from mid-2006 to early 2009, we identify 48 polar cap boundary crossings where the boundary can be simultaneously identified in auroral hiss from the RPWS electric field data, the density data from the RPWS/LP, and the CAPS/ELS data. We find that 22 of these crossings are in the northern hemisphere and 26 are in the southern hemisphere. CAPS densities are sometimes available, but the LP data provides a reasonable proxy, and the ELS spectrograms give much more information to help deduce the location of the spacecraft in the polar cap; see, for example, *Bunce et al*. [2008a] and *Jasinski et al*. [2014]. We find that clear transitions (like those shown in Figure 2a) through the northern and southern boundary regions cannot be observed in the remaining high-latitude orbits (constituting ~50 further polar cap boundary crossings in both hemispheres) because, in some cases, the characteristic step up in the frequency of the auroral hiss in the RPWS instrument data is not clear enough to allow for identification of the boundary in that data set. In those cases, the typical V-shaped auroral hiss features associated with upward propagating whistler mode emission from the auroral regions are obscured by more burst-like low-frequency emissions, not unlike that of terrestrial auroral hiss [*Kopf et al*., 2010].

In 32 of the 48 cases used in this study (15 in the northern hemisphere and 17 in the southern hemisphere), we are also able to observe the polar cap boundary in the ratio of electron intensities from the MIMI/LEMMS telescopes. We do not have LEMMS data for every case in this study because a clear observation of the boundary in the LEMMS telescopes requires that the spacecraft's attitude is such that the instrument channels are appropriately orientated with respect to the magnetic field lines during the period when Cassini crossed through the boundary region, which is not always the case for the polar cap boundary crossings during the high-latitude orbits. For each interval, we have considered the range of pitch angle coverage; we do not include cases where the pitch angles of the LEMMS channels are close to 90° (~75–105°) in the boundary crossing region. We also consider the clarity of the boundary signature in the line intensity plots; even if the pitch angle coverage is good, the boundary is not always clear (e.g., some suffer from elevated backgrounds from sunlight contamination and are therefore not definitive about open field). In this study we use channels E0 and E0* to identify the boundary in our 32 relevant cases. E0* is a linear combination of three C channels, summing to an energy range equal to that detected by channel E0, i.e., 110 to 365 keV. This allows for the most accurate identification of the polar cap boundary in the anisotropy of the electron intensities at these energies. We now present some examples of the polar cap boundary crossings considered in this study.

2.1. Typical Observations of the Polar Cap Boundary at High Latitudes

Figure 1 shows the spacecraft trajectory from one of the orbits from 2008, corresponding to Cassini revolution (Rev) 62, for days 81–85 inclusive. Figure 1a shows the orbit of Cassini projected onto the *X-Y* equatorial plane, while Figure 1b shows the orbit projected onto the *X-Z* meridional plane, in a coordinate system where the *Z* axis is aligned with the Saturn's rotation axis, and the *X-Z* plane contains the Sun. The trajectory is shown as a solid line marked with dots at the start of each "day of year" (DOY). On day 83 (part of which is highlighted in green), as Cassini underwent its periapsis pass on the nightside of the planet, the spacecraft crossed from high northern latitudes in the premidnight sector to high southern latitudes in the

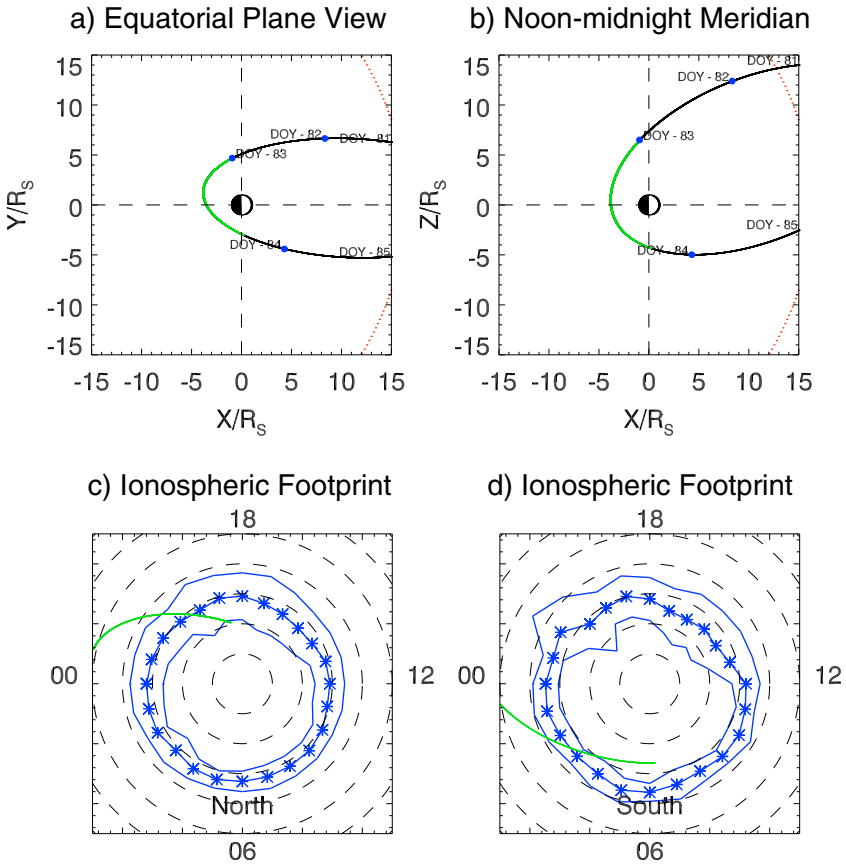

Figure 1. Cassini trajectory plots for Rev 62. (a) The orbit of Cassini in the *X-Y* equatorial plane in the KGS coordinate system where the *Z* axis is aligned with the Saturn's rotation axis, and the *X-Z* plane contains the Sun. The trajectory is shown as a solid line marked with dots at the start of each "day of year" (DOY). (b) The orbit in the *X-Z* meridional plane in the same coordinate system. An interval on DOY 83 is highlighted in green in Figures 1a and 1b corresponding to the time interval shown in Figure 2a. (c) Cassini's northern hemisphere trajectory on DOY 83 mapped along field lines into the northern ionosphere and projected onto a polar view with dotted circles every 5°. (d) The southern hemisphere trajectory for Cassini's pass on DOY 83 mapped to the southern ionosphere in the same form as Figure 1c. The green intervals in Figures 1c and 1d correspond to the northern and southern parts of the green intervals in Figures 1a and 1b.

postmidnight sector, via an equatorial crossing at ~10 UT at a local time of ~23 h and a radial distance of ~4 R_S (Saturn's equatorial radius R_S is 60,268 km). Figure 1c shows Cassini's northern hemisphere trajectory on DOY 83 mapped along field lines into the northern ionosphere, projected onto a polar view with dashed circles every 5°. Figure 1d similarly shows the southern hemisphere trajectory mapped to the southern ionosphere in the same format. The mapping employs the Cassini Saturn Orbit Insertion (SOI) internal planetary field model of *Dougherty et al*. [2005] and a typical ring current model of *Bunce et al*. [2008b] (corresponding to a subsolar magnetopause radius of 21 R_S). The blue lines in Figures 1c and 1d indicate the location and general morphology of the northern and southern UV aurora observed from 2007 to 2009 by Cassini's Ultraviolet Imaging Spectrograph (UVIS), the connected asterisks indicate the locations of the centroid maxima in auroral intensity colatitude profiles, and the solid lines poleward and equatorward of these maxima represent the full width at half maximum boundaries [*Carbary*, 2012]. Overall, the Cassini ionospheric footprint shows that the spacecraft made rapid traversals of the nightside auroral regions both inbound and outbound. The orbits throughout the high-latitude phase were broadly similar to Rev 62, where Cassini crossed the polar cap boundary in both hemispheres, within approximately half a planetary rotation and at similar nightside local times.

In Figure 2a we show a multi-instrument plot of 18 h of Cassini data on 2008 DOY 83 (from 0000 UT to 1800 UT) during Rev 62, which exemplifies the typical traversals of the polar cap boundary regions in Saturn's northern and southern hemispheres, seen in 43 of our 48 cases. The interval of time plotted here is that highlighted in

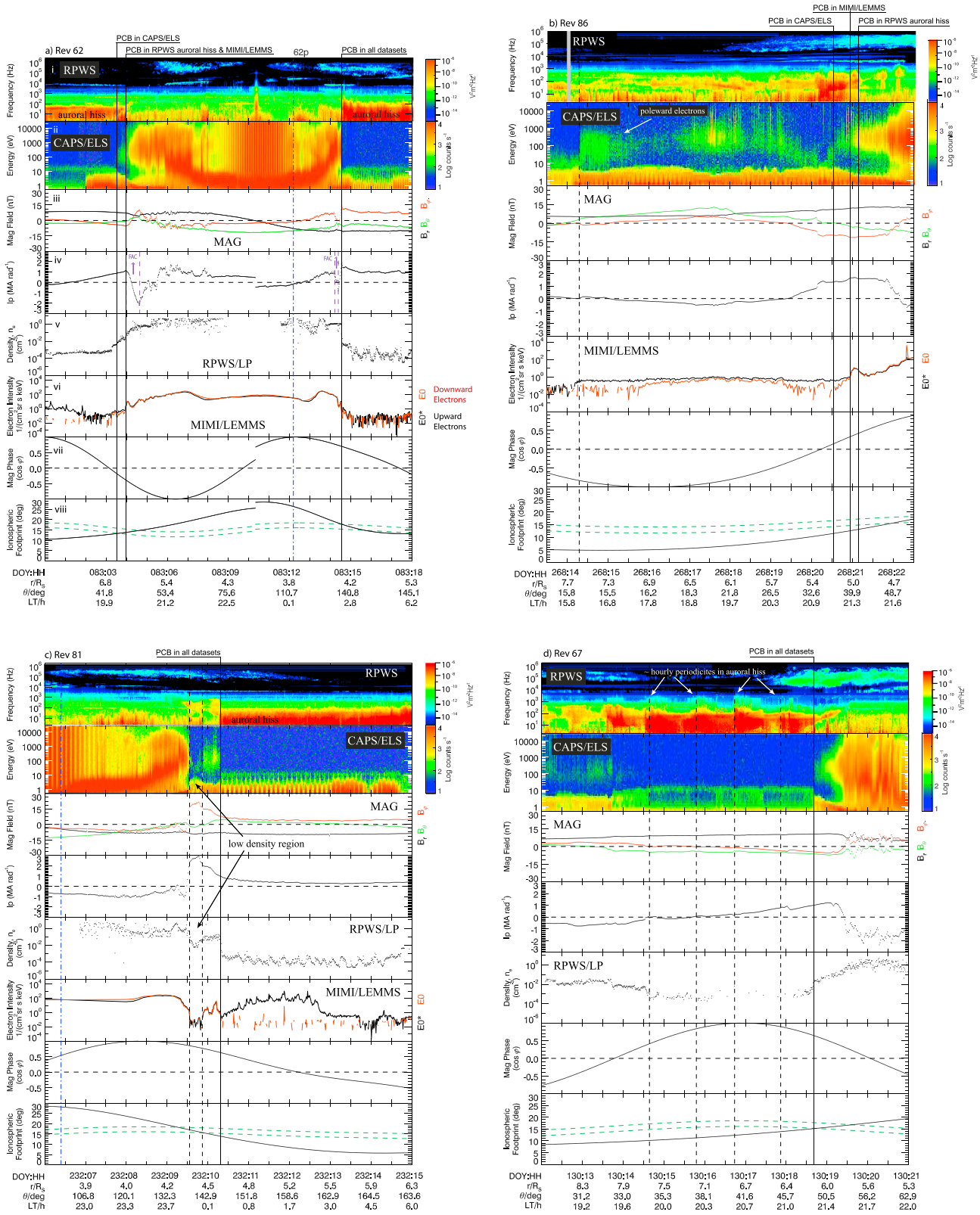

Figure 2

green in Figures 1a and 1b. Figure 2ai shows RPWS electric field data, where auroral hiss can be seen up to ~100 Hz and SKR above a few hundred kHz. At ~0400 UT and ~1430 UT, clear examples of Saturnian auroral hiss with the characteristic upper cutoff near the electron plasma frequency can be seen as the spacecraft traverses through the polar cap boundaries. Figure 2aii shows measurements of CAPS/ELS thermal electrons in the energy range 0.5 eV to 28 keV (from CAPS/ELS anode 5). Weak fluxes of cool ~10–100 eV electrons, excluding spacecraft photoelectrons, are presumed to be of magnetosheath origin. At the start of the interval (on DOY 83), the spacecraft was located at high latitudes in the northern hemisphere, where an absence of electrons above a few tens of eV can be observed in the ELS spectrogram. At ~0400 UT, we observe a transition of the electron population through a magnetosheath-like region (10–100 eV plasma electrons) to warm electrons (100–10,000 eV) characteristic of the outer magnetosphere, i.e., on closed field lines. At ~1430 UT, in the southern hemisphere, we observe a sharper transition of a warm electron population, through the magnetosheath region, into the polar cap region "void" of warm electrons. Figure 2aiii shows the three components of the magnetic field in spherical polar coordinates referenced to the planet's spin and magnetic axis from which the Cassini SOI model of the planetary field have been subtracted [*Dougherty et al*., 2005]; B_r, B_θ, and B_φ measured in units of nT. The radial and colatitude components reflect mainly the effect of the ring current. From the azimuthal component of the field, the Pedersen current I_P measured in MA rad^{-1} (Figure 2aiv) can be determined through application of equation (1) (a comprehensive explanation can be found in *Talboys et al*. [2009a], *Bunce et al*. [2008a], and *Bunce* [2012]). Therefore, the direction of the field-aligned currents can be identified from the latitude gradient of I_P, with the upward field-aligned currents outlined on Figure 2aiv by purple dashed lines and labelled as FAC. Figure 2av shows the proxy electron density derived from the RPWS/LP measured in cm^{-3}. At ~0400 UT there is an observable step up in electron density from ~10^{-3} cm^{-3} in the polar cap to ~1 cm^{-3} in the closed outer magnetosphere. At ~1430 UT there is a similar, but sharper, step down back to polar cap densities. *Morooka et al*. [2009] explain their method of using the floating potential of the LP (U_{float}) as a proxy to evaluate the local electron number density (when the ambient density falls below ~5 cm^{-3}). They calibrated U_{float} using CAPS/ELS data obtained during Cassini Saturn Orbit Insertion (SOI) and correct their LP density estimate for spacecraft attitude using an empirical function. Figure 2avi shows the upward (channel E0*) and downward (channel E0) field-aligned electron intensities from LEMMS measured in cm^{-2} sr^{-1} s^{-1} keV^{-1}. Where the two intensities equate (between ~0400 UT and ~1430 UT), it is indicative of a magnetically trapped electron population, i.e., on closed field lines. Figure 2avii shows the cosine of the magnetosphere planetary period oscillation phase of

Figure 2. Cassini multi-instrument plots of polar cap boundary region crossings during periapsis passes. (a) A Cassini multi-instrument plot of the polar cap boundary region crossings during the periapsis pass on Rev 62 (from 0000 UT to 1800 UT during 2008 DOY 83). Figure 2ai shows RPWS electric field data over frequency range 0–2 MHz, where auroral hiss can be observed up to ~100 Hz, and SKR emission above a few hundred kHz. Figure 2aii shows a CAPS/ELS color-coded electron spectrogram of energy range 0–30 keV. Figure 2aiii shows the three components of the magnetic field in spherical polar coordinates; B_r, B_θ, and B_φ (nT). Figure 2aiv shows the meridional ionospheric Pedersen current measured in MA rad^{-1}. The regions of upward field-aligned current are outlined by purple dashed lines and labelled as "FAC." Figure 2av shows the electron density measured by the RPWS Langmuir Probe (cm^{-3}). Figure 2avi shows the 110–365 keV upward (channel E0*) and downward (channel E0) field-aligned electron intensities measured by LEMMS (cm^{-2} sr^{-1} s^{-1} keV^{-1}). Figure 2avii shows the cosine of the planetary period oscillation (PPO) phase for each hemisphere calculated using the phase model of the preequinox southern summer planetary period magnetic field oscillations presented by *Andrews et al*. [2012]. Figure 2aviii shows the ionospheric colatitude of the spacecraft mapped to the relevant hemisphere. The green dashed lines indicate the typical location of the poleward and equatorward edges of the aurora varying with planetary period magnetic field oscillation phase with a 2.2° colatitude amplitude. (b) Multi-instrument data for the northern boundary crossing during Rev 86 (between 1330 UT and 2230 UT during 2008 DOY 268) where hot poleward electrons can be observed in the CAPS/ELS data (second panel down). (c) Multi-instrument data for the southern boundary crossing during Rev 81 (between 0600 UT and 1500 UT during 2008 DOY 232) where multiple transitions through a density boundary can be observed in the CAPS/ELS data (second panel down) and a region of high-intensity upward electrons can be seen just beyond the boundary in the polar cap region in the E0* electron intensity channel from LEMMS (sixth panel down). (d) Multi-instrument data for the northern boundary crossing during Rev 67 (between 1200 UT and 2100 UT during 2008 DOY 130) where approximately hourly periodicities can be observed in auroral hiss emissions and magnetic field data poleward of the polar cap boundary. The vertical dashed lines in Figure 2d highlight the downward field-aligned current region and mark where we observe periodic peaks in the frequency of auroral hiss emissions (in the first panel) simultaneously with perturbations in the B_θ and B_φ components of the magnetic field (in the third panel).

the relevant hemisphere, calculated using the phase model of the preequinox southern summer planetary period magnetic field oscillations presented by *Andrews et al*. [2012]. Finally, Figure 2aviii shows the ionospheric colatitude for the relevant hemisphere. Spacecraft position is shown at the bottom of the plot, specifically distance from Saturn (in R_S), latitude, and local time.

The green dashed lines in Figure 2aviii indicate the typical location of the poleward and equatorward edges of the auroral oval (13.9° and 16.3°, respectively) varying with the PPO phase of the relevant hemisphere with an ~2.2° colatitude amplitude. The latter amplitude is based upon the work by *Nichols et al*. [2008] who presented analysis of UV auroral images from the Hubble Space Telescope (HST) showing that the center of the southern auroral oval oscillates close to the period of the PPO. *Nichols et al*. [2008] described the motion of the center of the southern oval as an elongated ellipse along the prenoon to premidnight direction, of semimajor axis ~1.4° colatitude for aurora observed during January 2007 and ~2.2° for February 2008. *Nichols et al*. [2008] suggested that these oscillations are due to the presence of a rotating external current system, similar to that discussed by *Provan et al*. [2009b].

As we read the plot from left to right, the first black vertical line in Figure 2a marks where the northern polar cap boundary is observed in the CAPS/ELS electron data at 0332 UT, and then ~0.6° colatitude farther equatorward of that location (~26 min UT later), the boundary is observed simultaneously in both the cutoff in the RPWS auroral hiss and in the anisotropy of the E0 and E0* MIMI/LEMMS electron intensities (i.e., where the black and red LEMMS observations become equal, indicating equivalence in downward and upward directed electrons, respectively), indicated by the second vertical black line. A gradual step up in electron density is observed in Figure 2av over the boundary region encompassed by the two vertical lines. The polar cap boundary in the northern hemisphere on Rev 62 then is centered on 13.6° colatitude between the two distinct location identifications measured, first by CAPS/ELS 0.6° poleward of the simultaneous measurement by MIMI/LEMMS and RPWS auroral hiss.

In the southern hemisphere, the identification of the polar cap boundary is marked by the third black vertical line in Figure 2a at 1431 UT and is seen to be concurrently observed in the RPWS auroral hiss, the CAPS/ELS electron data and the MIMI/LEMMS electron channels and observed by a sharp step down in electron density. In the southern hemisphere in this example, the polar cap boundary resides at 17.9° southern colatitude in all indicators. Typical boundary crossings like those in the northern and southern crossings of Rev 62 were observed during ~90% of the 48 identified polar cap crossings. Further discussion of the polar cap boundary colocation (or otherwise) between the in situ data sets will be given in section 3, along with an evaluation of their relationship to the auroral field-aligned currents and the PPO phases.

2.2. Unusual Observations of the Polar Cap Boundary at High Latitudes

In most cases studied here the polar cap boundary crossings are clear like the "typical" case Rev 62 shown in Figure 2a. However, in a minority of cases (5 of the 48) we observed some interesting features in the various data sets, which led us to categorize them as unusual. Among these unusual examples is the singular case of the northern polar cap boundary crossing near dusk during Rev 86 where we see an electron population located poleward of the polar cap boundary extending up to 5° colatitude in the CAPS/ELS data. Figure 2b shows the multi-instrument data for the northern boundary crossing during Rev 86 (between 1330 UT and 2230 UT during 2008 DOY 268). We suggest that the data here indicate that Cassini skirted the polar cap boundary, remaining close to it for most of this interval, but without making a very rapid crossing. The spacecraft may be skirting the boundary due to a small motion of the boundary associated with the planetary period oscillation phase, as seen in Rev 99 by *Bunce et al*. [2014]. Black lines mark where we have identified the polar cap boundary (PCB) in the various data sets where the spacecraft appears to definitively move onto closed field lines. Interestingly in this example, at ~2000 UT, we observe a colder population of electrons in the CAPS/ELS spectrogram that could be related to a cusp population, as described by *Jasinski et al*. [2014].

The multi-instrument data for the southern boundary crossing during Rev 81 (between 0600 UT and 1500 UT during 2008 DOY 232) shown in Figure 2c, typifies a distinct category of unusual polar cap boundary crossings that are included in this study. In this case Cassini appears to make multiple separate transitions from high to low density as it moves poleward, as can also be seen in the LP data. These multiple transitions are observed 4 times in the 2006–2009 interval, in two boundary crossings in the northern hemisphere passes of Revs 32

and 59, and in two boundary crossings in the southern hemisphere passes of Revs 81 and 86. In these cases, we mark (solid black line) the polar cap boundary at the poleward edge of the multiple crossings, i.e., the last exit into the polar cap proper in each case. The dashed black lines equatorward of this indicate the possible earlier crossings in this example, discussed above. During the Rev 81 example (shown in Figure 2c), a region of high-intensity upward directed electrons is also observed poleward of the boundary in the polar cap region in the E0* electron intensity channel from LEMMS. These examples of multiple crossings are likely to be associated with short timescale polar cap boundary dynamics. Given that the local time of these observations is close to midnight, it may be associated with magnetotail dynamics [e.g., *Jackman et al*., 2011].

In addition to the ~10.8 h planetary period modulation seen in both the high-frequency SKR emission and auroral hiss emission, we have also found many examples of approximately hourly periodicities in the B_θ and B_φ components of the magnetic field and in the auroral hiss emissions poleward of the polar cap boundary. Such variations are found in ~50% of the boundary regions studied. An example of these approximately hourly periodicities can be seen in the multi-instrument data for the northern boundary crossing during Rev 67 (between 1200 UT and 2100 UT during 2008 DOY 130) in Figure 2d. The solid black line marks the polar cap boundary (PCB) in the various data sets. The dashed black lines highlight the generally downward field-aligned current region (evidence by the consistently increasing Pedersen current as the spacecraft moves toward the equator) and mark where we observe approximately hourly periodic peaks in the frequency of auroral hiss emissions (in the first panel) simultaneously with associated perturbations mainly in the B_θ and B_φ components of the magnetic field (in the third panel). *Mitchell et al*. [2009] reported on similar period pulses of particle acceleration events, which were consistently observed in various Cassini data sets, including electrostatic noise seen in the RPWS data. *Mitchell et al*. [2009] attribute these pulsed events to transient downward field-aligned current structures and pulses of whistler mode noise. They note that this type of emission is always observed close to bright, upward current regions in the auroral zone at Earth. *Badman et al*. [2012] suggested that pulsed events of field-aligned ion beams with a modulation of ~1 h may be related to pulsed reconnection. *Badman et al*. [2012] and *Bunce et al*. [2014] noted that these approximately hourly pulsed events are observed in the downward FAC regions only, which is consistent with our study. We highlight this as an interesting topic for future study but pursue it no further in this paper as it does not directly affect the identification of the polar cap boundary.

3. Results

3.1. Polar Cap Boundary and Field-Aligned Current Locations

The 0.6° colatitude difference between the polar cap boundary signature in the CAPS/ELS data and the simultaneous LEMMS and RPWS signatures, found in the Rev 62 northern hemisphere boundary crossing in Figure 2a, is larger than the average value from our 48 examples. The average value is found to be 0.34° ± 0.05°. In ~50% of cases the polar cap boundary was identified at the same colatitude in all data sets within error (i.e., ± 0.05° colatitude). In all cases the boundary was observed simultaneously to within 2.7° ± 0.05° colatitude. We then take the center of each determined polar cap boundary region to be the middle point between the maximum and the minimum colatitudes of individual boundaries in each hemisphere. The center point and width of the upward field-aligned current region was also recorded in each case and compared to the associated polar cap boundary. The average poleward edge location of the upward current could then be directly compared to the average location of the polar cap boundary to infer the average separation of the main auroral oval (poleward edge) and the polar cap boundary.

Figure 3 shows the location of all 48 of (a) the northern and (b) the southern polar cap boundaries (PCBs) observed in the RPWS auroral hiss emission (circles), CAPS/ELS electrons (plus symbols), and in the anisotropy of the MIMI/LEMMS channels (cross symbols) for each boundary crossing included in the study. Figure 3 illustrates that in most cases (~50%), the polar cap boundary was identified at the same colatitude in all three data sets. In the cases where the polar cap boundary was not observed simultaneously in all three data sets, the boundary was generally observed first in CAPS/ELS and second in auroral hiss when moving from high to low latitudes (low to high colatitudes).

Figure 4 shows the southern colatitude of the center of the polar cap boundary (dark grey circles) and the region of the upward field-aligned current (grey bars) for each polar cap boundary (PCB) crossing included in the study. It can immediately be seen from Figure 4 that the polar cap boundary is not observed at a

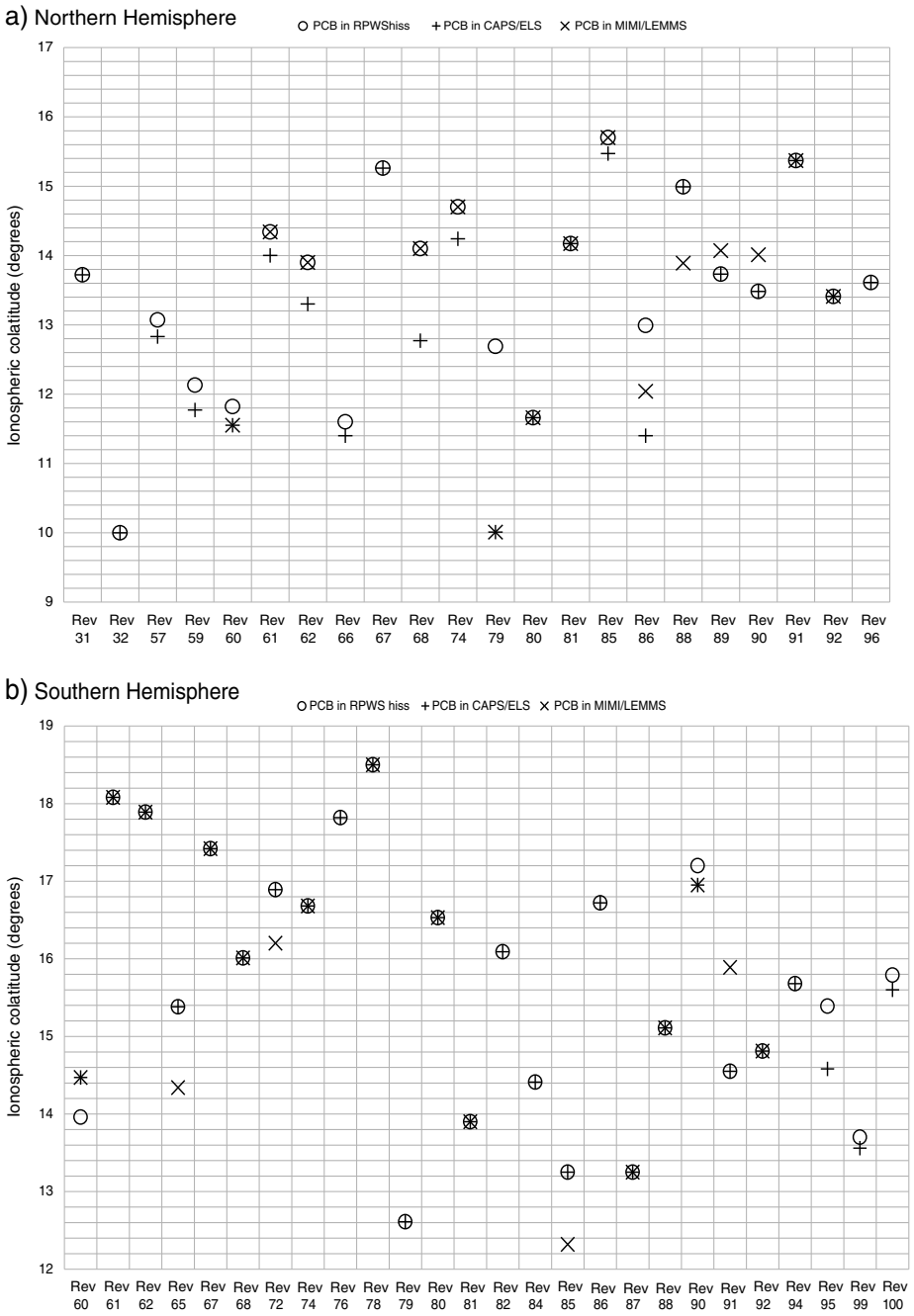

Figure 3. (a) Northern and (b) southern colatitudes of the polar cap boundary (PCB) observed in the RPWS auroral hiss emission (circles), CAPS/ELS electrons (plus symbols), and in the anisotropy of the MIMI/LEMMS channels (cross symbols) for each boundary crossing included in the study.

constant colatitude and that the boundary and upward field-aligned current (FAC) region are not colocated, which is in agreement with the conclusion of *Talboys et al*. [2011] that the polar cap boundary from the CAPS/ELS measurements is consistently poleward of the upward field-aligned current region inferred from the magnetic field measurements. The average location of the polar cap boundary in the south, as marked in Figure 4 by a solid horizontal line, is at 15.6° colatitude. The range of colatitudes in the southern hemisphere is 5.9°, with the most poleward example seen at 12.6° colatitude and the most equatorward recording at 18.5° colatitude. The displacement between the polar cap boundary and the poleward edge of the upward current region varies between 0.2° and 5.3° colatitude in the southern

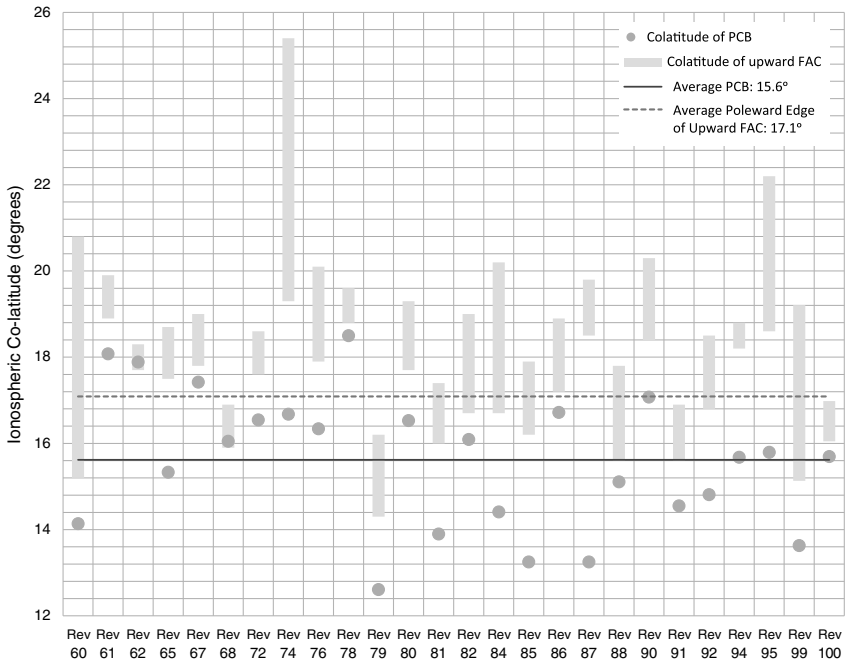

Figure 4. Southern colatitude of the center of the polar cap boundary (circles) and region of the upward field-aligned current (bars) for each boundary crossing.

hemisphere data. The average equatorward displacement of the poleward edge of the upward field-aligned current region from the polar cap boundary is 1.5° colatitude in the southern data. The average position of the poleward edge of the upward current region of 17.1° colatitude is marked in Figure 4 by a dashed horizontal line.

Figure 5 shows the equivalent plot for the northern boundary and field-aligned current locations in the same format as Figure 4. Again, it can be seen that the polar cap boundary is not observed at a constant value of colatitude in the northern hemisphere. The average location of the boundary in the north is at 13.3° colatitude as marked in Figure 5 by a solid horizontal line, the most poleward point is at

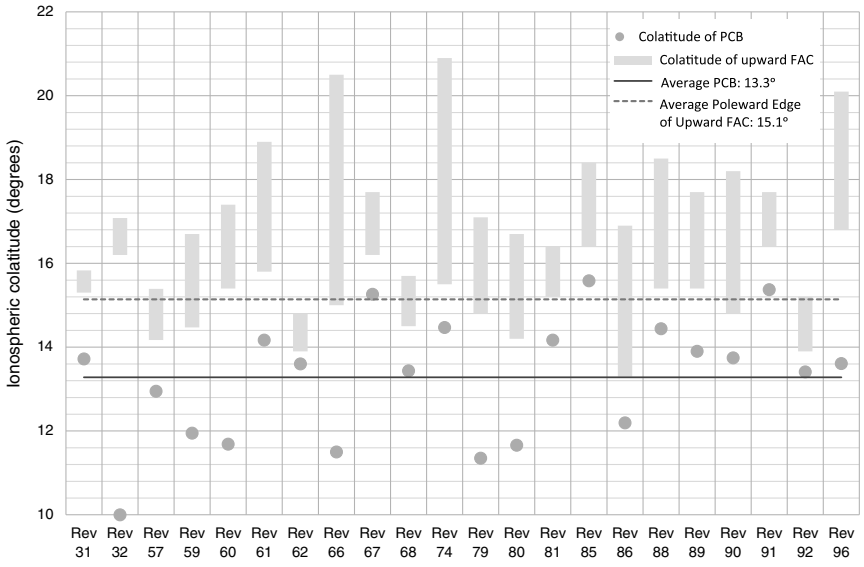

Figure 5. Northern colatitude of the center of the polar cap boundary (circles) and region of the upward field-aligned current (bars) for each boundary crossing.

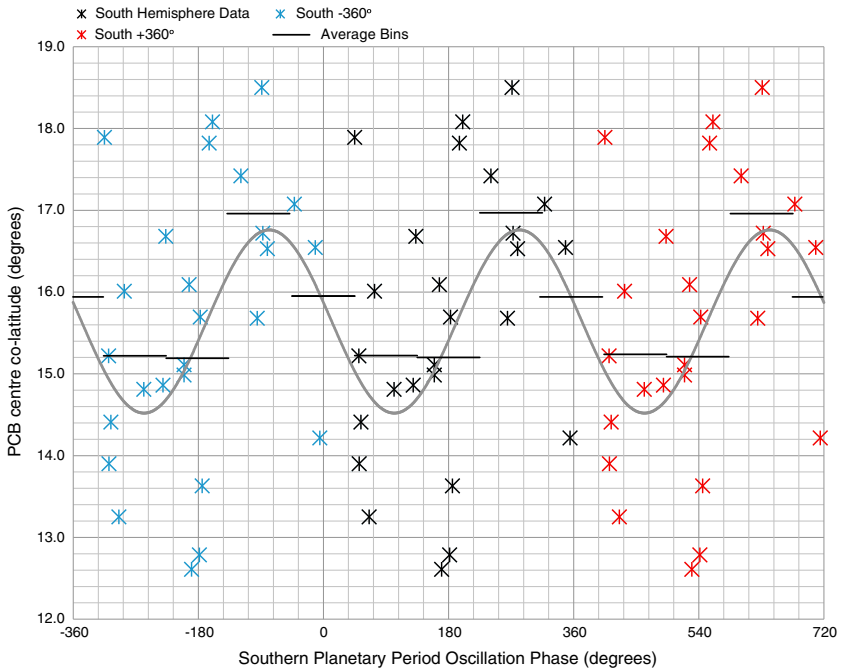

Figure 6. Southern colatitude of the polar cap boundary (PCB) versus the southern planetary period magnetic field oscillation phase for the southern hemisphere crossings. The black asterisks are from southern region crossings. The red points are the data repeated with +360°, and the blue data points are the data repeated with −360°. The black lines indicate average bins of colatitude. The grey line represents a best fit sinusoidal regression line.

10.0° colatitude, and the most equatorward point is at 15.6° colatitude (and thus a range of 5.6°, similar to the variation in the southern hemisphere). The displacement between the polar cap boundary and the poleward edge of the upward current region varies between 0.3° and 6.2° colatitude in the northern data. The average equatorward displacement of the poleward edge of the upward field-aligned current region from the polar cap boundary is 1.8° colatitude in the northern data. The average position of the poleward edge of the upward current region of 15.1° colatitude is marked in Figure 5 by a dashed horizontal line.

3.2. Planetary Period Magnetic Field Oscillation Phase Dependence of the Boundary

To assess if the polar cap boundary locations shows any dependence on the southern and northern PPO phase, we compare the colatitude positions from our 48 examples, separated into northern and southern cases, with a model of the phase of the planetary period oscillations according to the work of *Andrews et al.* [2012]. In Figure 6 we show the southern hemisphere polar cap boundary (PCB) locations (in colatitude) versus the southern planetary period oscillation phase. To emphasize the continuity of the data, three cycles of a phase are shown across the plot, such that each point is plotted 3 times. If the location of the southern polar cap boundary crossings varied solely as a function of the southern PPO phase, Figure 6 would likely display a clear periodic relationship, e.g., a sinusoid with an amplitude of ~2° colatitude according to the UV aurora study by *Nichols et al.* [2008] about the mean location (i.e., 15.6° southern colatitude found in section 3.1 above). However, no such relationship is obviously apparent. Therefore, we have binned the data into four groups of southern PPO phase centered about 0°, 90°, 180°, and 270° and averaged the colatitude of the polar cap boundary within each bin. This gives an indication of the possible ordering of the polar cap boundary position with phase. The mean southern colatitude of each "bin" of phase is shown in Figure 6. There is some indication here of a structured variation of the colatitude of the polar cap boundary, which is consistent with a sinusoidal variation (shown in Figure 6). However, a sinusoidal regression fit of the southern data has proved to be statistically insignificant. We therefore conclude that the data indicate that the location of the polar cap boundary is not exclusively ordered by the PPO phase in the southern hemisphere, and there must be other contributing factors. It therefore seems likely that the location of Saturn's polar cap boundary is associated with a combination of the PPO phase together with other processes, for

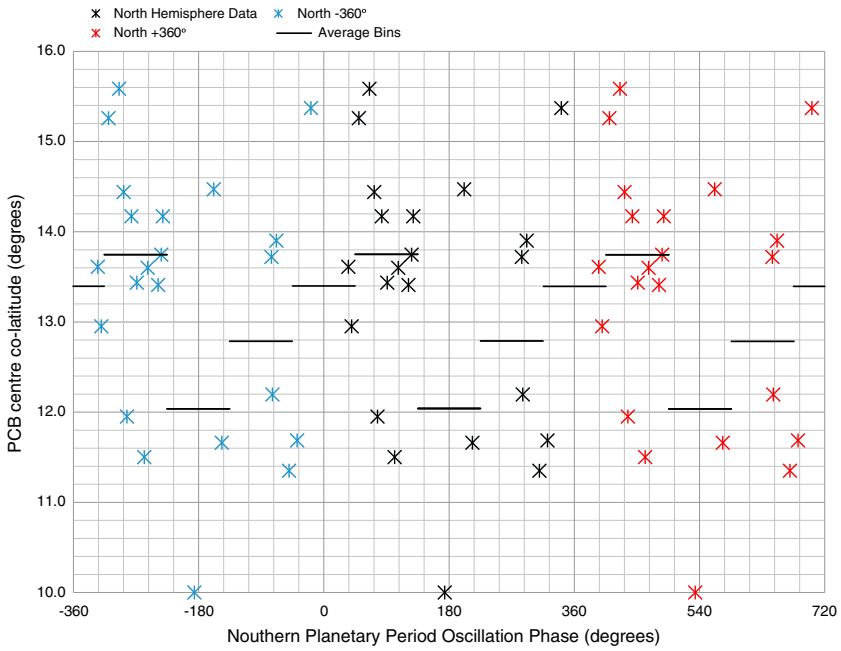

Figure 7. Northern colatitude of the polar cap boundary (PCB) versus the northern planetary period magnetic field oscillation phase for the northern hemisphere crossings. The black asterisks are from northern region crossings. The red data points are the data repeated with +360°, and the blue data points are the data repeated with −360°. The black lines indicate average bins of colatitude.

example, reconnection-driven processes associated with the solar wind interaction, as suggested by *Badman et al.* [2005, 2006, 2013] and *Radioti et al.* [2011, 2013].

Figure 7, in the same format as Figure 6, shows the northern PPO phase [*Andrews et al.*, 2012] versus the polar cap boundary locations observed in the northern hemisphere. There is less evidence of any ordering of the northern polar cap boundary locations with the northern PPO phase than there is in the southern data. However, we have binned the data into four groups of southern PPO phase centered about 0°, 90°, 180°, and 270° and averaged the colatitude of the polar cap boundary over each bin. This indicates that there is some ordering of the polar cap boundary position with phase. In recent studies [e.g., *Provan et al.*, 2009a], oscillations in the equatorial region have been found to be dominated by the southern period in the preequinox southern summer. Ordering our northern polar cap boundary colatitudes by the southern PPO phase has also shown no clear relationship. We suggest that the southern data are ordered by the southern period alone to some degree but that the northern data are influenced by a mixture of northern and southern PPO phase. This is likely to explain why a relationship with the oscillation phase in the northern data is even less clear than in the southern data.

4. Summary and Discussion

Here we have presented the first systematic investigation of the polar cap boundary in various in situ data sets for all the high-latitude boundary region crossings between 2006 and 2009. We have identified 48 polar cap crossings where the polar cap boundary can be observed in auroral hiss from the RPWS electric field data, the density data from the RPWS/LP, and the CAPS/ELS electron spectrograms. In 32 of our 48 cases, we also observe the polar cap boundary in the ratio of electron intensities from the LEMMS channels. In 5 of the 48 boundary crossings included in this study, we observed some unusual features in the various data sets including multiple crossings of the boundary, hot poleward electrons, and high-intensity upward flowing electrons observed just beyond the boundary in the E0* LEMMS channel. We have also observed approximately hourly periodicities in the auroral hiss in ~50% of the 48 boundary regions studied, comparable to those reported by *Mitchell et al.* [2009].

We have determined the level of coincidence of the polar cap boundary between the various in situ data sets to be 0.34° ± 0.05° colatitude. In 25 (~50%) of cases the polar cap boundary was identified at the

same colatitude in all data sets within error (i.e., ± 0.05° colatitude), at least across the range of local times studied here. As noted in the context of the Earth, the agreement between different proxies for the boundary can vary with magnetic local time [e.g., *Wild et al*., 2004]. The average location of the boundary in the southern hemisphere was found to be at 15.6° southern colatitude, with the average displacement of the poleward edge of the upward current region ~1.5° colatitude equatorward in the southern hemisphere data. The average location of the boundary in the northern hemisphere was found to be at 13.3° colatitude, with the average location of the poleward edge of the upward current region ~1.8° colatitude equatorward of the average northern boundary location. This is unlike the situation at Earth [e.g., *Clausen et al*., 2013]. They find that the upward directed Region 1 currents associated with the solar wind driving of the Earth's magnetosphere are in good agreement with the open-closed field line boundary determined from the cutoff in particle precipitation measured by the DMSP spacecraft.

We find the mean location of the poleward edge of the upward current region in the northern hemisphere to be at 15.1° ± 0.2° colatitude and the mean location of the poleward edge of the upward current region in the southern hemisphere to be at 17.1° ± 0.3° colatitude. We also find that the average width of the upward current region is ~ 2° colatitude in both hemispheres. *Carbary* [2012] presented analysis of UVIS images from 2007 to 2009 where the mean location of the peak intensity in auroral colatitude profiles of the northern and southern aurora were 15.1° ± 1.0° colatitude and 15.9° ± 1.9° colatitude, respectively, and the mean poleward aurora boundaries (determined from the half-maxima points) were ~ 2° poleward of the mean maxima in each hemisphere. They noted that in the UV auroral emissions, particularly the auroral equatorward boundaries, a shift is seen toward the pole around noon. Since more than 90% of the upward field-aligned currents measured in this study presented here were observed at local times close to midnight, these in situ results are not inconsistent with a nightside equatorward shift of the aurora. From images from Cassini's visual and infrared mapping spectrometer taken between 2006 and 2008, *Badman et al*. [2011] determined that Saturn's infrared northern aurora had a nearly circular shape with an average radius of 16.4° colatitude, centered 1.6° toward midnight, which is also consistent with results presented here.

There is some indication that the southern polar cap boundary is ordered by the southern PPO phase, but even if there was a variation of similar amplitude to the *Nichols et al*. [2008] variation, it is very noisy and no statistically significant variation emerges. There is no clear evidence of any ordering of the northern polar cap boundary locations with the northern PPO phase such that we cannot confidently say that the PPO phase has any clear control of the motion of the polar cap boundary in the northern hemisphere during this interval of data. The significance of magnetic flux flow involving magnetic reconnection in magnetospheric dynamics at the outer planets has been questioned; e.g., *Mauk et al*. [2009], *Delamere and Bagenal* [2013], *Desroche et al*. [2013], and *Masters et al*. [2012] proposed that conditions at Saturn's magnetopause are rarely favorable for permitting reconnection. However, there is some evidence of processes associated with magnetopause reconnection in various data sets [e.g., *McAndrews et al*., 2008; *Badman et al*., 2013; *Radioti et al*., 2011; *Lai et al*., 2012]. Therefore, we propose that in addition to any PPO-related motion of the polar cap boundary in this study, there is also motion associated with opening and closing of magnetic flux through the solar wind interaction with Saturn's magnetosphere.

Given 0.34° ± 0.05° colatitude level of confidence in the coincidence of the boundary location in the various data sets, one instrument data set could now be used to identify the boundary with a known level of agreement. Since CAPS/ELS data are not available for Cassini's 2013/2014 high-latitude orbits, establishing the level of coincidence will be useful for identifying the polar cap boundary in future studies. Our study has shown that the region of upward field-aligned current associated with the aurora is clearly separated from the polar cap boundary in both hemispheres by ~1.5–1.8°. This will have an impact on various related fields of study. For example, *Badman et al*.'s [2005] investigation of the flux in Saturn's open region used the poleward edge of ultraviolet aurora from 68 HST images from 2004 to identify the "open-closed" boundary, whereas we have discovered that the polar cap boundary is typically located ~1.5–1.8° poleward of the aurora-producing currents. This difference would be equivalent to a difference of ~20% (~8 GWb) in the amount of open flux typically present in Saturn's magnetosphere (for a polar cap boundary location of 15.6° colatitude), which would therefore need to be taken into consideration when estimating the open flux present in the magnetosphere from, e.g., auroral images.

Acknowledgments
S.L.J. is supported by an STFC PhD Studentship. E.J.B., S.W.H.C., G.P., and T.K.Y. are supported by the 500 STFC Leicester Consolidated grant ST/K001000/1, and E.J.B. by a Philip Leverhulme award. C.S.A. supported by a Royal Society University Research Fellowship. Thanks to G.R. Lewis and L.K. Gilbert for data reduction of CAPS/ELS data and thanks to S. Kellock and the Cassini team at Imperial College for MAG data processing. All Cassini data from 2006 to 2009 are available from the Planetary Data System (https://pds.jpl.nasa.gov/).

Michael Liemohn thanks two anonymous reviewers for their assistance in evaluating this paper.

References

Andrews, D. J., S. W. H. Cowley, M. K. Dougherty, and G. Provan (2010), Magnetic field oscillations near the planetary period in Saturn's equatorial magnetosphere: Variation of amplitude and phase with radial distance and local time, *J. Geophys. Res.*, *115*, A04212, doi:10.1029/2009JA014729.

Andrews, D. J., S. W. H. Cowley, M. K. Dougherty, L. Lamy, G. Provan, and D. J. Southwood (2012), Planetary period oscillations in Saturn's magnetosphere: Evolution of magnetic oscillation properties from southern summer to postequinox, *J. Geophys. Res.*, *117*, A04224, doi:10.1029/2011JA017444.

Badman, S. V., E. J. Bunce, J. T. Clarke, S. W. H. Cowley, J.-C. Ge´rard, D. Grodent, and S. E. Milan (2005), Open flux estimates in Saturn's magnetosphere during the January 2004 Cassini-HST campaign, and implications for reconnection rates, *J. Geophys. Res.*, *110*, A11216, doi:10.1029/2005JA011240.

Badman, S. V., S. W. H. Cowley, J. C. Gerard, and D. Grodent (2006), A statistical analysis of the location and width of Saturn's southern auroras, *Ann. Geophys.*, *24*, 3533–3545, doi:10.5194/ANGEO-24-3533-2006.

Badman, S. V., N. Achilleos, K. H. Baines, R. H. Brown, E. J. Bunce, M. K. Dougherty, H. Melin, J. D. Nichols, and T. Stallard (2011), Location of Saturn's northern infrared aurora determined from Cassini VIMS images, *Geophys. Res. Lett.*, *38*, L03102, doi:10.1029/2010GL046193.

Badman, S. V., et al. (2012), Cassini observations of ion and electron beams at Saturn and their relationship to infrared auroral arcs, *J. Geophys. Res.*, *117*, A01211, doi:10.1029/2011JA017222.

Badman, S. V., A. Masters, H. Hasegawa, M. Fujimoto, A. Radioti, D. Grodent, N. Sergis, M. K. Dougherty, and A. J. Coates (2013), Bursty magnetic reconnection at Saturn's magnetopause, *Geophys. Res. Lett.*, *40*, 1027–1031, doi:10.1002/grl.50199.

Bunce, E. J. (2012), Origins of Saturn's auroral emissions and their relationship to large-scale magnetosphere dynamics, in *Auroral Phenomenology and Magnetospheric Processes: Earth and Other Planets*, edited by A. Keiling et al., AGU, Washington, D. C., doi:10.1029/2011GM001191.

Bunce, E. J., et al. (2008a), Origin of Saturn's aurora: Simultaneous observations by Cassini and the Hubble Space Telescope, *J. Geophys. Res.*, *113*, A09209, doi:10.1029/2008JA013257.

Bunce, E. J., C. S. Arridge, S. W. H. Cowley, and M. K. Dougherty (2008b), Magnetic field structure of Saturn's dayside magnetosphere and its mapping to the ionosphere: Results from ring-current modeling, *J. Geophys. Res.*, *113*, A02207, doi:10.1029/2007JA012538.

Bunce, E. J., et al. (2014), Cassini nightside observations of the oscillatory motion of Saturn's northern auroral oval, *J. Geophys. Res. Space Physics*, *119*, 3528–3543, doi:10.1002/2013JA019527.

Carbary, J. F. (2012), The morphology of Saturn's ultraviolet aurora, *J. Geophys. Res.*, *117*, A06210, doi:10.1029/2012JA017670.

Carbary, J. F., and D. G. Mitchell (2013), Periodicities in Saturn's magnetosphere, *Rev. Geophys.*, *51*, 1–30, doi:10.1002/rog.20006.

Carbary, J. F., and D. G. Mitchell (2014), Keogram analysis of ENA images at Saturn, *J. Geophys. Res. Space Physics*, *119*, 1771–1780, doi:10.1002/2014JA019784.

Chisham, G., M. P. Freeman, and T. Sotirelis (2004), A statistical comparison of SuperDARN spectral width boundaries and DMSP particle precipitation boundaries in the nightside ionosphere, *Geophys. Res. Lett.*, *31*, doi:10.1029/2003GL019074.

Clausen, L. B. N., J. B. H. Baker, J. M. Ruohoniemi, S. E. Milan, J. C. Coxon, S. Wing, S. Ohtani, and B. J. Anderson (2013), Temporal and spatial dynamics of the regions 1 and 2 Birkeland currents during substorms, *J. Geophys. Res. Space Physics*, *118*, 3007–3016, doi:10.1002/jgra.50288.

Cowley, S. W. H., and M. Lockwood (1992), Excitation and decay of solar wind-driven flows in the magnetosphere-ionosphere system, *Ann. Geophys.*, *10*, 103–115.

Cowley, S. W. H., and M. Lockwood (1996), Time-dependent flows in the coupled solar wind-magnetosphere-ionosphere system, *Adv. Space Res.*, *18*, 141–150.

Cowley, S. W. H., E. J. Bunce, and R. Prangé (2004), Saturn's polar ionospheric flows and their relation to the main auroral oval, *Ann. Geophys.*, *22*, 1379–1394, doi:10.5194/angeo-22-1379-2004.

Cowley, S. W. H., C. S. Arridge, E. J. Bunce, J. T. Clarke, A. J. Coates, M. K. Dougherty, J. C. Gerard, D. Grodent, J. D. Nichols, and D. L. Talboys (2008), Auroral current systems in Saturn's magnetosphere: Comparison of theoretical models with Cassini and HST observations, *Ann. Geophys.*, *26*, 2613–2630, doi:10.5194/ANGEO-26-2613-2008.

Delamere, P. A., and F. Bagenal (2013), Magnetotail structure of the giant magnetospheres: Implications of the viscous interaction with the solar wind, *J. Geophys. Res. Space Physics*, *118*, 7045–7053, doi:10.1002/2013JA019179.

Desroche, M., F. Bagenal, P. A. Delamere, and N. Erkaev (2013), Conditions at the magnetopause of Saturn and implications for the solar wind interaction, *J. Geophys. Res. Space Physics*, *118*, 3087–3095, doi:10.1002/jgra.50294.

Dougherty, M. K., et al. (2005), Cassini magnetometer observations during Saturn orbit insertion, *Science*, *307*, 1266–1270, doi:10.1126/science.1106098.

Dungey, J. W. (1961), Interplanetary field and the auroral zones, *Phys. Rev. Lett.*, *6*, 47–48, doi:10.1103/PhysRevLett.6.47.

Evans, L. C., and E. C. Stone (1972), Electron polar cap and the boundary of open geomagnetic field lines, *J. Geophys. Res.*, *77*, 5580–5585, doi:10.1029/JA077i028p05580.

Gurnett, D. A. (1966), A satellite study of VLF hiss, *J. Geophys. Res.*, *71*(23), 5599–5615, doi:10.1029/JZ071i023p05599.

Gurnett, D. A., A. Lecacheux, W. S. Kurth, A. M. Persoon, J. B. Groene, L. Lamy, P. Zarka, and J. F. Carbary (2009), Discovery of a north-south asymmetry in Saturn's radio rotation period, *Geophys. Res. Lett.*, *36*, L21108, doi:10.1029/2009GL040774.

Gurnett, D. A., et al. (2010), A plasmapause-like density boundary at high latitudes in Saturn's magnetosphere, *Geophys. Res. Lett.*, *37*, L16806, doi:10.1029/2010GL044466.

Gurnett, D. A., A. M. Persoon, J. B. Groene, W. S. Kurth, M. Morooka, J. E. Wahlund, and J. D. Nichols (2011), The rotation of the plasmapause-like boundary at high latitudes in Saturn's magnetosphere and its relation to the eccentric rotation of the northern and southern auroral ovals, *Geophys. Res. Lett.*, *38*, L21203, doi:10.1029/2011GL049547.

Hill, T. W. (1979), Inertial limit on corotation, *J. Geophys. Res.*, *84*, 6554–6558, doi:10.1029/JA084iA11p06554.

Hubert, B., A. T. Aikio, O. Amm, T. Pitkanen, K. Kauristie, S. E. Milan, S. W. H. Cowley, and J.-C. Gerard (2010), Comparison of the open-closed field line boundary location inferred using IMAGE-FUV SI12 images and EISCAT radar observations, *Ann. Geophys.*, *28*, 883–892.

Isbell, J., A. J. Dessler, and J. H. Waite Jr. (1984), Magnetospheric energization by interaction between planetary spin and the solar wind, *J. Geophys. Res.*, *89*(A12), 10, 716–10,722, doi:10.1029/JA089iA12p10716.

Jackman, C. M., J. A. Slavin, and S. W. H. Cowley (2011), Cassini observations of plasmoid structure and dynamics: Implications for the role of magnetic reconnection in magnetospheric circulation at Saturn, *J. Geophys. Res.*, *116*, A10212, doi:10.1029/2011JA016682.

Jasinski, J. M., et al. (2014), Cusp observation at Saturn's high-latitude magnetosphere by the Cassini spacecraft, *Geophys. Res. Lett.*, *41*, 1382–1388, doi:10.1002/2014GL059319.

Kasahara, Y., K. Yoshida, T. Matsuo, I. Kimura, and T. Mukai (1995), Propagation characteristics of auroral hiss observed by Akebono satellite, *J. Geomagn. Geoelec.*, *47*, 509–525.

Kopf, A. J., et al. (2010), Electron beams as the source of whistler-mode auroral hiss at Saturn, *Geophys. Res. Lett.*, *37*, L09102, doi:10.1029/2010GL042980.

Lai, H. R., H. Y. Wei, C. T. Russell, C. S. Arridge, and M. K. Dougherty (2012), Reconnection at the magnetopause of Saturn: Perspective from FTE occurrence and magnetosphere size, *J. Geophys. Res.*, *117*, A05222, doi:10.1029/2011JA017263.

Lamy, L. (2011), Variability of southern and northern periodicities, in *Planetary Radio Emissions VII*, edited by H. O. Rucker et al., pp. 39–50, Austrian Academy of Sciences, Vienna, Austria.

Masters, A., J. P. Eastwood, M. Swisdak, M. F. Thomsen, C. T. Russell, N. Sergis, F. J. Crary, M. K. Dougherty, A. J. Coates, and S. M. Krimigis (2012), The importance of plasma β conditions for magnetic reconnection at Saturn's magnetopause, *Geophys. Res. Lett.*, *39*, L08103, doi:10.1029/2012GL051372.

Mauk, B. H., et al. (2009), Fundamental plasma processes in Saturn's magnetosphere, in *Saturn From Cassini-Huygens*, p. 281, Springer, Netherlands, doi:10.1007/978-1-4020-9217-6-11.

McAndrews, H. J., et al. (2008), Evidence for reconnection at Saturn's magnetopause, *J. Geophys. Res.*, *113*, A04210, doi:10.1029/2007JA012581.

Milan, S. E., M. Lester, S. W. H. Cowley, K. Oksavik, M. Brittnacher, R. A. Greenwald, G. Sofko, and J.-P. Villain (2003), Variations in polar cap area during two substorm cycles, *Ann. Geophys.*, *21*, 1121–1140.

Mitchell, D. G., W. S. Kurth, G. B. Hospodarsky, N. Krupp, J. Saur, B. H. Mauk, J. F. Carbary, S. M. Krimigis, M. K. Dougherty, and D. C. Hamilton (2009), Ion conics and electron beams associated with auroral processes on Saturn, *J. Geophys. Res.*, *114*, A02212, doi:10.1029/2008JA013621.

Morooka, M. W., et al. (2009), The electron density of Saturn's magnetosphere, *Ann. Geophys.*, *27*, 2971–2991, doi:10.5194/angeo-27-2971-2009.

Müller, A. L., J. Saur, N. Krupp, E. Roussos, B. H. Mauk, A. M. Rymer, D. G. Mitchell, and S. M. Krimigis (2010), Azimuthal plasma flow in the Kronian magnetosphere, *J. Geophys. Res.*, *115*, A08203, doi:10.1029/2009JA015122.

Nichols, J. D., J. T. Clarke, S. W. H. Cowley, J. Duval, A. J. Farmer, J.-C. Gérard, D. Grodent, and S. Wannawichian (2008), The oscillation of Saturn's southern auroral oval, *J. Geophys. Res.*, *113*, A11205, doi:10.1029/2008JA013444.

Persoon, A. M., D. A. Gurnett, W. K. Peterson, J. H. Waite Jr., J. L. Burch, and J. L. Green (1988), Electron density depletions in the nightside auroral zone, *J. Geophys. Res.*, *93*, 1871–1895, doi:10.1029/JA093iA03p01871.

Provan, G., D. J. Andrews, C. S. Arridge, A. J. Coates, S. W. H. Cowley, S. E. Milan, M. K. Dougherty, and D. M. Wright (2009a), Polarization and phase of planetary-period magnetic field oscillations on high-latitude field lines in Saturn's magnetosphere, *J. Geophys. Res.*, *114*, A02225, doi:10.1029/2008JA013782.

Provan, G., S. W. H. Cowley, and J. D. Nichols (2009b), Phase relation of oscillations near the planetary period of Saturn's auroral oval and the equatorial magnetospheric magnetic field, *J. Geophys. Res.*, *114*, A04205, doi:10.1029/2008JA013988.

Provan, G., D. J. Andrews, B. Cecconi, S. W. H. Cowley, M. K. Dougherty, L. Lamy, and P. Zarka (2011), Magnetospheric period magnetic field oscillations at Saturn: Equatorial phase "jitter" produced by superposition of southern- and northern-period oscillations, *J. Geophys. Res.*, *116*, A04225, doi:10.1029/2010JA016213.

Radioti, A., D. Grodent, J.-C. Gérard, S. E. Milan, B. Bonfond, J. Gustin, and W. Pryor (2011), Bifurcations of the main auroral ring at Saturn: Ionospheric signatures of consecutive reconnection events at the magnetopause, *J. Geophys. Res.*, *116*, A11209, doi:10.1029/2011JA016661.

Radioti, A., D. Grodent, J.-C. Gérard, B. Bonfond, J. Gustin, W. Pryor, J. M. Jasinski, and C. S. Arridge (2013), Auroral signatures of multiple magnetopause reconnection at Saturn, *Geophys. Res. Lett.*, *40*, 4498–4502, doi:10.1002/grl.50889.

Schippers, P., N. André, D. A. Gurnett, G. R. Lewis, A. M. Persoon, and A. J. Coates (2012), Identification of electron field-aligned current systems in Saturn's magnetosphere, *J. Geophys. Res.*, *117*, A05204, doi:10.1029/2011JA017352.

Siscoe, G. L., and T. S. Huang (1985), Polar cap inflation and deflation, *J. Geophys. Res.*, *90*, 543–547, doi:10.1029/JA090iA01p00543.

Stallard, T. S., S. Miller, L. A. Trafton, T. R. Geballe, and R. D. Joseph (2004), Ion winds in Saturn's southern auroral/polar region, *Icarus*, *167*(1), 204–211, doi:10.1016/j.icarus.2003.09.006.

Talboys, D. L., C. S. Arridge, E. J. Bunce, A. J. Coates, S. W. H. Cowley, and M. K. Dougherty (2009a), Characterization of auroral current systems in Saturn's magnetosphere: High-latitude Cassini observations, *J. Geophys. Res.*, *114*, A06220, doi:10.1029/2008JA013846.

Talboys, D. L., C. S. Arridge, E. J. Bunce, A. J. Coates, S. W. H. Cowley, M. K. Dougherty, and K. K. Khurana (2009b), Signatures of field-aligned currents in Saturn's nightside magnetosphere, *Geophys. Res. Lett.*, *36*, L19107, doi:10.1029/2009GL039867.

Talboys, D. L., E. J. Bunce, S. W. H. Cowley, C. S. Arridge, A. J. Coates, and M. K. Dougherty (2011), Statistical characteristics of field-aligned currents in Saturn's nightside magnetosphere, *J. Geophys. Res.*, *116*, A04213, doi:10.1029/2010JA016102.

Thomsen, M. F., C. M. Jackman, R. L. Tokar, and R. J. Wilson (2014), Plasma flows in Saturn's nightside magnetosphere, *J. Geophys. Res. Space Physics*, *119*, 4521–4535, doi:10.1002/2014JA019912.

Vasyliunas, V. M. (1983), Plasma distribution and flow, in *Physics of the Jovian Magnetosphere*, edited by A. J. Dessler, pp. 395–453, Cambridge Univ. Press, New York.

Wild, J. A., S. E. Milan, C. J. Owen, J. M. Bosqued, M. Lester, D. M. Wright, H. Frey, C. W. Carlson, A. N. Fazakerley, and H. Reme (2004), The location of the open-closed magnetic field line boundary in the dawn sector auroral ionosphere, *Ann. Geophys.*, *22*, 3625–3639.

Wilson, R. J., R. L. Tokar, and M. G. Henderson (2009), Thermal ion flow in Saturn's inner magnetosphere measured by the Cassini plasma spectrometer: A signature of the Enceladus torus?, *Geophys. Res. Lett.*, *36*, L23104, doi:10.1029/2009GL040225.